Journal of Solid State Chemistry **155,** 292–297 (2000)
doi:10.1006/jssc.2000.8887, available online at http://www.idealibrary.com on IDEAL®

Structure Analysis of A-Type Carbonate Apatite by a Single-Crystal X-Ray Diffraction Method

Yasushi Suetsugu,* Yasuhiko Takahashi,† Fujio P. Okamura,* and Junzo Tanaka*

**National Institute for Research in Inorganic Materials, 1-1 Namiki, Tsukuba, Ibaraki 305-0044, Japan, and †Institute of Applied Physics, University of Tsukuba, 1-1 Tennodai, Tsukuba, Ibaraki 305-0006, Japan*

Received April 9, 1999; in revised form July 13, 2000; accepted July 27, 2000; published online November 29, 2000

The crystal structure of carbonate apatite was determined by X-ray diffraction analysis with $R_w = 0.027$ using a single crystal grown by a $CaCO_3$ flux method. The chemical formula of the crystal was $Ca_{9.75}[(PO_4)_{5.5}(CO_3)_{0.5}]CO_3$, in which all the A sites corresponding to OH sites in hydroxyapatite were substituted by CO_3 ions. The space group was $P\bar{6}$ (hexagonal) with lattice parameters of $a = 0.9480(3)$ nm and $c = 0.6898(1)$ nm. The triangular plane of the CO_3 ion substituting the A site randomly occupied one of six equivalent sites around the $\bar{6}$ axis parallel to the *c*-axis; one of three C–O bonds of CO_3 lay on the $\bar{6}$ axis. The quantitative relation between CO_3 ions in the A (OH) site and B (PO_4) site of the present crystal was accounted for via Ca deficiency. © 2000 Academic Press

1. INTRODUCTION

Carbonate apatite (hereafter CAp) has drawn substantial attention from not only mineralogical but also biological points of view. Especially, as the inorganic component of vertebrate's hard tissue is analogous to carbonate-containing hydroxyapatite (1, 2), the elucidation of its crystal structure is fundamental for the understanding of bone remodeling *in vivo*.

It is possible for a CO_3 ion to replace two different sites in hydroxyapatite ($Ca_{10}(PO_4)_6(OH)_2$, HAp). One is in the OH ion site (channel site) and the other is in the PO_4 site, called A and B site, respectively (3). The chemical formula of the carbonate-containing HAp is formally given by $Ca_{10-x/2}[(PO_4)_{6-x}(CO_3)_x]\ [(OH)_{2-2y}(CO_3)_y]$ on the basis of a simple charge neutrality. Though a lot of structural studies on this compound have been performed, the precise configuration of carbonate ions in HAp has not been determined yet, due to the difficulty in preparing sufficient large single crystals for an X-ray structure analysis.

In the previous paper (4), single crystals of CAp with $y = 1$ were successfully grown by a $CaCO_3$ flux method, and the space group of CAp was determined to be $P\bar{6}$. In addition, it was elucidated from polarized FT-IR measurements that the triangular plane of a CO_3 ion was parallel to the *c*-axis for the A-site substitution and perpendicular to the *c*-axis for the B-site substitution.

In the present paper, we performed X-ray structure analyses for the CAp single crystals, and the precise configuration of the A-site substituted CO_3 ions was determined based on X-ray diffraction data collected using a four-circle X-ray diffractometer. Further, it was shown that the amount of the B-site substituted CO_3 ions was correlated with that of the A-site substituted CO_3 ions via the formation of Ca deficiencies.

2. EXPERIMENTAL PROCEDURE

CAp crystals were grown using a $CaCO_3$ flux method (4). The crystals obtained were hexagonal prismatic and their chemical composition was determined from EPMA analyses together with the results of FT-IR spectra to be $Ca_{9.75}[(PO_4)_{5.5}(CO_3)_{0.5}]CO_3$, in which all the A sites and about $\frac{1}{12}$ of the B sites were occupied by CO_3 ions (4).

A CAp crystal of 200 μm in diameter was mounted on the top of a glass fiber and set on a four-circle diffractometer (Rigaku AFC-5R). X-ray diffraction data were measured at room temperature with HOPG monochromated Ag$K\alpha$ (40 kV, 180 mA) irradiated from a rotating anode. X-ray diffraction data were collected for $-19 \le h \le 19$, $-19 \le k \le 19$, and $-14 \le l \le 14$ using a $2\theta-\omega$ scan technique. Unique reflections whose intensities were larger than σ were 1574, where σ is a standard deviation. Reflections with so large intensities that they might cause damage to the counter were measured with the attenuator and corrected afterward. Lattice parameters were refined by a least squares method using 25 diffraction peaks automatically searched and centered by the diffractometer.

Calculations for structure analyses were undertaken using a Xtal set of programs (5) based on the space group $P\bar{6}$ (4). The atomic scattering factors and the anomalous dispersion factors were taken from Ref. 6. Since the amount of the

0022-4596/00 $35.00

B-site substituted CO_3 ions, i.e., $\frac{1}{12}$, was sufficiently low for structure factors to be not significantly influenced, the chemical formula of the crystal was approximated at $Ca_{10}(PO_4)_6CO_3$. In the calculations, initial positions for the Ca and PO_4 ions were taken from HAp data after Hughes *et al.* (7). After refining the positional parameters of Ca and PO_4 ions, unknown positions for the A-site CO_3 ion were determined by referring to differential (D)-Fourier electron density maps and weighed *R* factors. Finally, the positions for all the constituents were refined by a full-matrix least square method.

3. RESULTS AND DISCUSSION

3.1. The Cell Parameters of CAp

Table 1 shows crystal data for the present crystal together with a pure HAp crystal (8) and a powder of completely substituted A-type CAp (9). The unit cell parameter *a* for the present crystal was larger than that for the pure HAp and smaller than that for the A-type CAp powder. In general, it is considered that the parameter *a* increases when the CO_3 ions substitute the A sites (OH), while it decreases when the CO_3 ions substitute the B sites (PO_4) because of difference in ionic size. The A sites in the present crystal were perfectly substituted by the CO_3 ions and the B sites were partially substituted by them; therefore, the parameter *a* took a middle point of the pure HAp and the A-type CAp powder.

The cell parameter *c* for the present crystal was larger in comparison with the pure HAp and the A-type CAp powder. The slight increase in the *c*-axis together with the increment of the B-site CO_3 was consistent with a previous report (10). Though the detailed mechanism about the change of the *c*-axis length was not given in Ref. 10, the substitution of a CO_3^{2-} ion for a PO_4^{3-} ion could induce $\frac{1}{2}$ deficiency of Ca^{2+} to maintain the charge neutrality. It was therefore conjectured that the Ca deficiency slightly increased a repulsive force between anions like PO_4^{3-} and OH^- ions, resulting in the increase in the length of the *c*-axis.

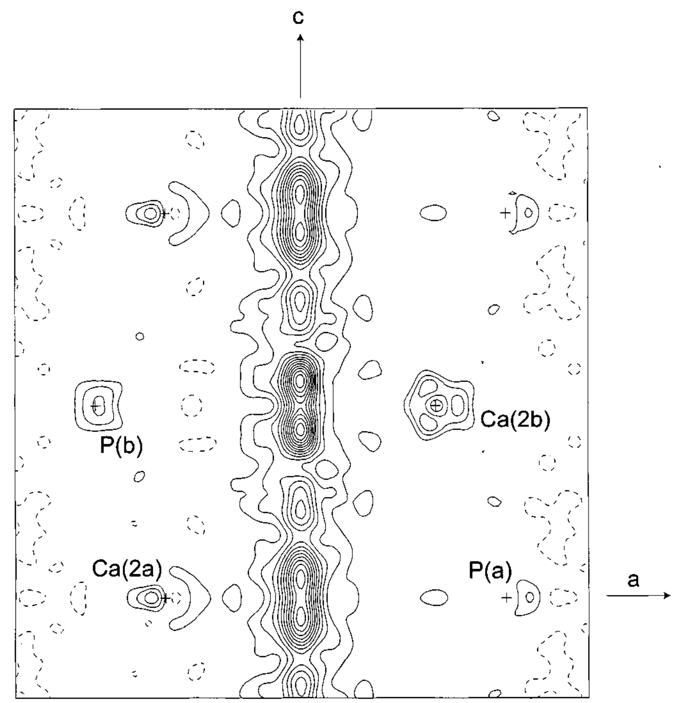

FIG. 1. The D-Fourier map of electron density in CAp after the refinement for Ca and PO_4 without CO_3. The contour is represented on the (010) plane and the interval of lines is 500/nm^3. Atoms within 0.03 nm from this plane are given. Solid and broken lines correspond to positive and negative values, respectively.

3.2. The Determination of CAp Crystal Structure

Figure 1 shows a D-Fourier contour after the positions for the Ca and PO_4 ions were refined without CO_3 ion. The contour is represented on the (010) plane. The interval between the lines is $5 \times 10^2/\text{nm}^3$ in electron density (solid lines stand for a positive value and broken lines for a negative value).

In Fig. 1, the electron density had two peaks at ($x = 0$, $y = 0$, $z = 0.24$) and (0, 0, 0.05); other peaks appeared at

TABLE 1
The Comparison of Crystal Data for CAp and HAp

	The present work: CAp	HAp	A-type CAp (powder)
Chemical formulae	$Ca_{9.75}[(PO_4)_{5.5}(CO_3)_{0.5}]CO_3$	$Ca_{10}(PO_4)_6(OH)_2$	$Ca_{10}(PO_4)_6CO_3$
Space group	$P\bar{6}$	$P2_1/b$	Pb
a (nm)	0.9480(3)	0.9418	0.9557(3)
b (nm)	0.9480(3)	2a	2a
c (nm)	0.6898(1)	0.6881	0.6872(2)
γ (°)	120	120	120.36(4)
Z	1	2	2

Note. Data for HAp are Ref. 8 and data for powdered CAp are from Ref. 9.

their equivalent positions. These peaks corresponded to the A-site CO_3 ion whose C and O atoms could alternatively occupy either site of (0, 0, 0.24) and (0, 0, 0.05). Taking the D-Fourier and the corresponding R factor into account, it was most plausible that the C atom was located at (0, 0, 0.24) and the O atom at (0, 0, 0.05). In this case, one of C–O bonds lay on the $\bar{6}$ axis. The configuration was consistent with the result of polarized infrared spectra measurement (4) that a triangular plane of CO_3 in the A site was parallel to the c-axis.

A distance between C and O was estimated to be about 0.13 nm, very close to the bond length of C–O observed for many carbonate compounds. Further, the peak heights in the D-Fourier approximately coincided to the electron densities of C and O. Therefore, the initial coordinate parameters of C and one of three Os were set at (0, 0, 0.24) and (0, 0, 0.05), respectively.

Figure 2 shows the D-Fourier contour after refinement of parameters for all the constituents including CO_3 by a full-matrix least squares calculation, projected on the (010) plane. The resultant weighed R factor was 0.027, and only small residues were correspondingly found in Fig. 2. This result indicated that the structure calculated was sufficiently appropriate for the present CAp crystal.

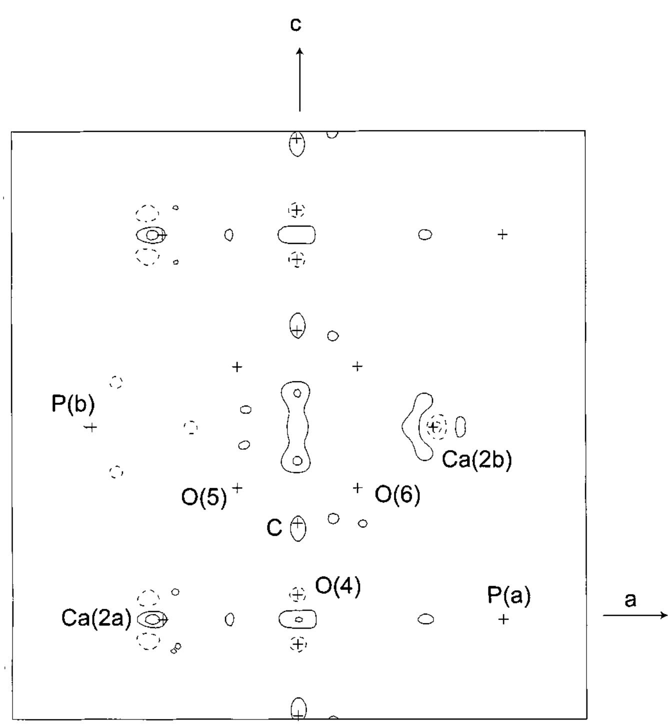

FIG. 2. The D-Fourier map of electron density in CAp after the refinement for all constituents of Ca, PO_4, and CO_3. The contour is represented on the (010) plane and the interval of lines is 500/nm^3. Atoms within 0.03 nm from this plane are given. Solid and broken lines correspond to positive and negative values, respectively.

TABLE 2
Positional Parameters of CAp

	Occupancy	x	y	z
Ca(1a)	1.02	$\frac{2}{3}$	$\frac{1}{3}$	0.2487(2)
Ca(1b)	0.89	$\frac{1}{3}$	$\frac{2}{3}$	0.2538(2)
Ca(2a)	0.96	0.7517(2)	0.7410(2)	0
Ca(2b)	0.95	0.2497(2)	0.2608(2)	$\frac{1}{2}$
P(a)	0.95	0.3708(3)	0.4019(3)	0
P(b)	0.89	0.6285(3)	0.5985(3)	$\frac{1}{2}$
O(1a)	1.17	0.4853(7)	0.3326(7)	0
O(1b)	0.84	0.5157(7)	0.6712(7)	$\frac{1}{2}$
O(2a)	0.97	0.4623(8)	0.5875(7)	0
O(2b)	1.05	0.5305(8)	0.4154(9)	$\frac{1}{2}$
O(3a)	0.83	0.2611(6)	0.3542(7)	0.1828(5)
O(3b)	1.11	0.7377(7)	0.6606(8)	0.3283(5)
C	0.54	0	0	0.2491(15)
O(4)	0.55	0	0	0.0642(14)
O(5)	0.18	0.1249(13)	0.0239(29)	0.3418(19)
O(6)	0.18	− 0.1271(16)	− 0.0276(48)	0.3411(21)

In the least-square calculation, the C–O distances, and the O–C–O angles were restrained within 0.5% deviation from 0.128 nm and 120°, respectively, to prevent unreasonable distortion of a CO_3 triangle of only light atoms. Without such restriction, the distances and angles were often deviated and the thermal parameters became extensively large.

Table 2 shows the positional parameters refined for all the atoms. In the case where the space group was $P6_3/m$ (7), the numbers of independent positions for Ca, P, and O in the PO_4 ion are 2, 1, and 3, respectively. However, as the space group of the present crystal was $P\bar{6}$ with a lower symmetry in comparison with $P6_3/m$, Ca(2) and PO_4 were classified into two groups corresponding to the sites which located near an apex (suffix a) or a base (suffix b) of the CO_3 triangle (see Fig. 3). The notation of the atoms used here was the same as that of $P6_3/m$ to be easily compared, for example, Ca(2a) and Ca(2b) of $P\bar{6}$ to Ca(2) of $P6_3/m$. Ca(1) was also divided into two groups, but they were equivalent regarding the positional relation with CO_3; then, their suffixs (a and b) are merely for convenience. As regards the c-axis, the plane of $z = 0$ in $P\bar{6}$ was shifted to $z = -\frac{1}{4}$ in $P6_3/m$ because of the requirement of description of symmetry.

Figures 3 and 4 show the atomic configuration projected on the (010) and (001) planes, respectively. In this configuration, six equivalent positions were allowed for the CO_3 ion at the A site in a unit cell, which were located around the $\bar{6}$ axis. A set of three positions in six equivalent positions were mutually produced from another set with mirror planes at $z = 0$ and $\frac{1}{2}$ perpendicular to the c-axis. These six equivalent positions were statistically occupied by the CO_3 ion to allow the symmetry of the space group $P\bar{6}$ to be satisfied.

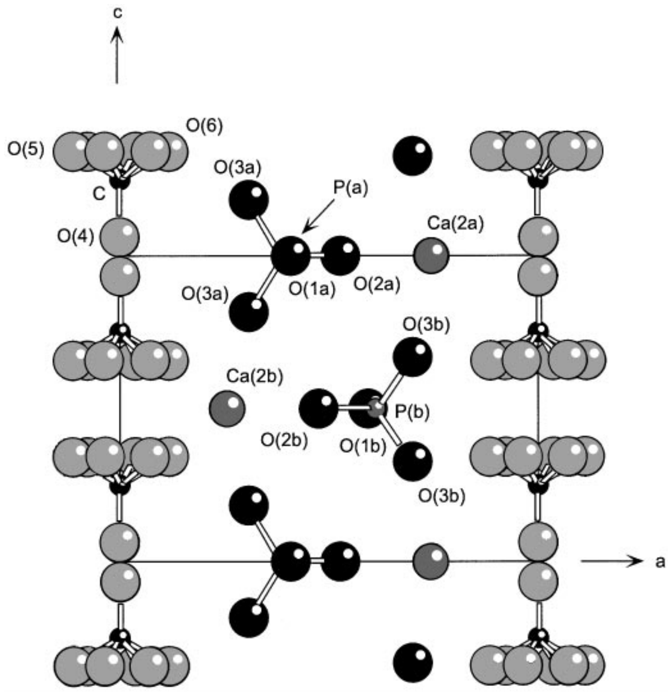

FIG. 3. The atomic configuration in CAp projected on the (010) plane.

3.3. *Local Ionic Configurations and Thermal Parameters*

Table 3 gives bond lengths and angles formed in the CAp structure. As for the PO_4 ion existing near the base of the A-site CO_3 ion, the distance P(b)–O(3b) was smaller than that of hydroxyapatite (7). In addition, the apparent PO_4 site had a small bond length for O(3b)–O(3b) and a small angle for O(3b)–P(b)–O(3b). These results indicated that the PO_4 tetrahedron was compressed along the *c*-axis; the reason was partly due to the influence of adjacent O(5) or O(6) ions; however, a more important factor was possibly a disregard for the B-site CO_3 which actually substituted $\frac{1}{12}$ of PO_4 ions.

While a substantially small value of the angle O(2a)–P(a)–O(3a) and consequently large value of O(1a)–P(a)–O(3a) indicate that O(3a) tends to be distant from O(6) by repulsion, O(3b) does not have such tendency, which is probably because of CO_3 ions actually substituting this site.

These features of the interatomic lengths and angles regarding PO_4 ion can be explained if CO_3 ion is introduced into the B site near the base of A-site CO_3 predominantly compared to the B site near the apex of A-site CO_3 when the crystal was grown by the flux method.

The anisotropic thermal parameters evaluated are listed in Table 4. From this table, it was found that the thermal parameters for O(3b) was larger in comparison to O(3a). As reported in Ref. 4, when the CO_3 ion substituted the PO_4 ion (B site), the CO_3 ion was located for its triangular plane to be perpendicular to the *c*-axis. The large thermal parameters for O(3b) therefore indicated that the O(3b) site in PO_4 was missed when the CO_3 ions partially substituted the B site.

The CO_3 triangle at the A site, given in Table 3, was compressed within the *c*-plane as the bond lengths of C–O(5) and C–O(6) were less than that of C–O(4) and the

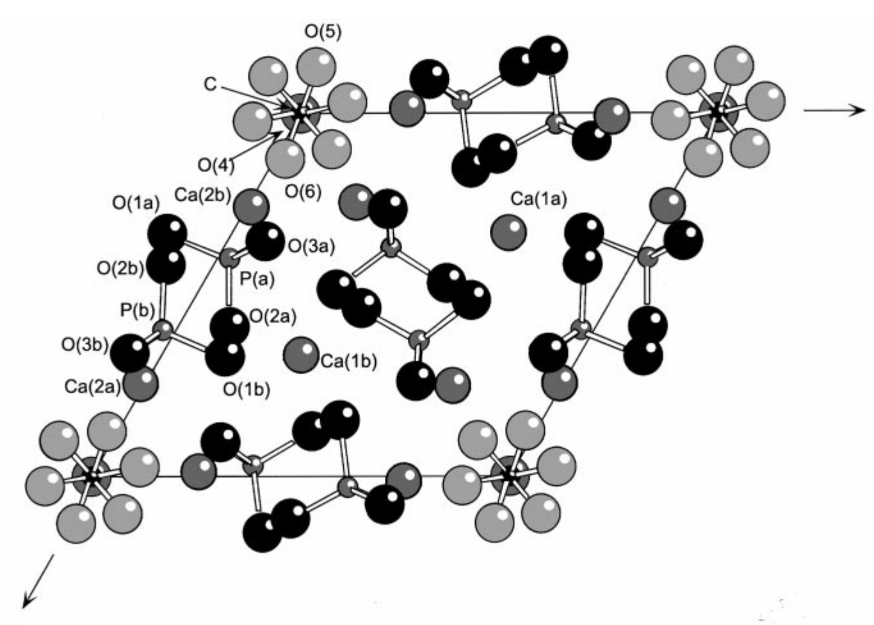

FIG. 4. The atomic configuration in CAp projected on the (001) plane.

TABLE 3
Interatomic Distance and Bond Angle of CAp

	CAp	σ	HAp
Phosphate tetrahedron			
P(a)–O(1a)	1.5238	0.0088	1.534
P(a)–O(2a)	1.5242	0.0061	1.537
P(a)–O(3a)	1.5515	0.0043	1.529
P(b)–O(1b)	1.5346	0.0111	
P(b)–O(2b)	1.5046	0.0162	
P(b)–O(3b)	1.4863	0.0119	
O(1a)–P(a)–O(2a)	112.38	0.38	111.041
O(1a)–P(a)–O(3a)	113.13	0.30	111.427
O(2a)–P(a)–O(3a)	104.35	0.30	107.509
O(3a)–P(a)–O(3a)	108.79	0.29	107.733
O(1b)–P(b)–O(2b)	110.55	0.54	
O(1b)–P(b)–O(3b)	109.03	0.57	
O(2b)–P(b)–O(3b)	111.25	0.83	
O(3b)–P(b)–O(3b)	105.58	0.85	
O(1a)–O(2a)	2.5325	0.0107	2.531
O(2a)–O(3a)	2.4294	0.0058	2.473
O(3a)–O(1a)	2.5664	0.0090	2.531
O(3a)–O(3a)	2.5228	0.0046	2.471
O(1b)–O(2b)	2.4980	0.0209	
O(2b)–O(3b)	2.4687	0.0095	
O(3b)–O(1b)	2.4600	0.0127	
O(3b)–O(3b)	2.3674	0.0050	
Carbonate triangle			
C–O(4)	1.2748	0.0143	
C–O(5)	1.2633	0.0157	
C–O(6)	1.2685	0.0207	
O(4)–C–O(5)	120.44	0.75	
O(5)–C–O(6)	119.52	1.30	
O(6)–C–O(4)	120.02	0.86	
Ca(2) triangle			
Ca(2a)–Ca(2a)	4.1664	0.0036	4.085
Ca(2b)–Ca(2b)	4.1950	0.0031	

Note. Data for HAp are from Ref. (7).

angle of O(5)–C–O(6) was smaller than the other angles like O(4)–C–O(5). This distortion suggested that a channel around the $\bar{6}$ axis was relatively narrow for the substitution of the CO_3 triangle.

The thermal parameters for O(5) and O(6) in CO_3 given in Table 4 were considerably large, while the thermal parameters for O(4) were small. This result was probably related to the fact that the occupation factor for the O(4) site on the $\bar{6}$ axis was $\frac{1}{2}$ and that for the O(5) and O(6) sites was $\frac{1}{6}$. A large value of U_{33} for C indicated an extensive thermal vibration along the c-axis.

Ca(2a) and Ca(2b) ions formed two types of triangles around the $\bar{6}$ axis near the apex and the base of the A site CO_3 triangle, respectively. Two triangles were different in size: the triangle of the Ca(2b) ions was slightly larger than that of the Ca(2a) ions. The large triangle for the former was due to the stereoscopic interaction between the Ca(2b) ions and the O(5)/O(6) ions in CO_3, corresponding to the distortion of the CO_3 triangle.

3.4. The Correlation of A- and B-site Substitution

The chemical formula of CAp is given by $Ca_{10-x/2}[(PO_4)_{6-x}(CO_3)_x](CO_3)$ based on a simple charge neutrality. As the B site is linked to the Ca site, the substitution of a CO_3 ion for the B site is necessarily accompanied with the formation of a half Ca deficiency. In this formula, parameter x is assumed to be independent. However, x was always constant around $x = \frac{1}{2}$ for the present crystal even if the growth conditions of CAp crystals were varied (11), implying that x is correlated to the content of CO_3 ion in the A site.

Here, based on the result of the structure analysis, we assume that the combinations of CO_3–CO_3 pair in the A site have four patterns shown in Figs. 5a–5d. The pattern in Fig. 5e occurs probably in very low probability because it requires the pattern in Fig. 5f somewhere for charge neutrality, which is obviously implausible to exist because two Os are located too closely. The state depicted in Fig. 5d is plausibly unstable because the surrounding three Ca ions directly face one another without a CO_3 ion among them; therefore, it is conjectured that that state is sufficiently unstable for the structure to be not maintained, resulting in the formation of a Ca deficiency. The Ca deficiency can cause two CO_3 ions to substitute two PO_4 ions due to the charge neutrality. If the four states in Figs. 5a–5d appear statistically in equal probabilities and therefore the

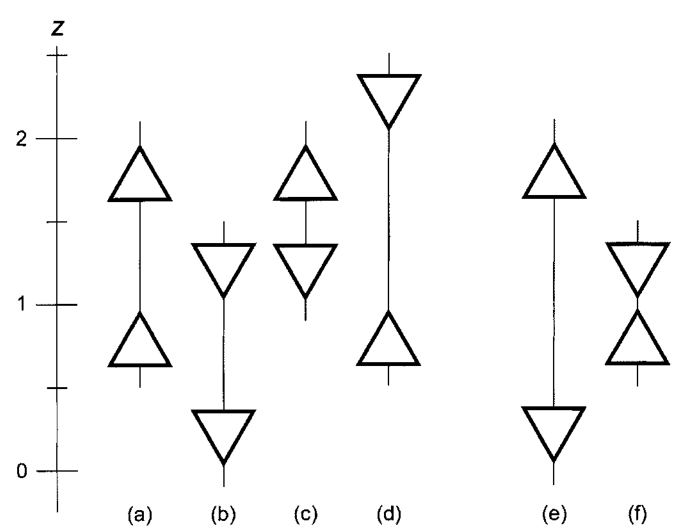

FIG. 5. Combination patterns of CO_3–CO_3 pair in the A site. Triangles represent CO_3 ions. Existence of pattern (e) or (f) is implausible.

TABLE 4
Anisotropic Thermal Parameters of CAp

	U_{11}	U_{22}	U_{33}	U_{12}	U_{13}	U_{23}
Ca(1a)	0.0200(5)	0.0200(5)	0.0082(3)	0.0100(2)	0	0
Ca(1b)	0.0184(6)	0.0184(6)	0.0188(5)	0.0092(3)	0	0
Ca(2a)	0.0317(10)	0.0328(11)	0.0249(6)	0.0215(9)	0	0
Ca(2b)	0.0250(8)	0.0258(8)	0.0142(4)	0.0161(7)	0	0
P(a)	0.0180(10)	0.0214(11)	0.0114(6)	0.0146(9)	0	0
P(b)	0.0168(10)	0.0156(10)	0.0111(6)	0.0096(8)	0	0
O(1a)	0.0348(27)	0.0451(28)	0.0222(19)	0.0291(23)	0	0
O(1b)	0.0128(20)	0.0124(18)	0.0166(18)	0.0100(16)	0	0
O(2a)	0.0210(24)	0.0133(21)	0.0794(47)	0.0061(19)	0	0
O(2b)	0.0373(33)	0.0402(34)	0.0913(53)	0.0291(29)	0	0
O(3a)	0.0302(18)	0.0560(23)	0.0143(11)	0.0347(18)	0.0123(11)	0.0138(12)
O(3b)	0.0751(29)	0.1359(40)	0.0447(19)	0.0859(31)	0.0344(20)	0.0518(23)
C	0.0694(67)	0.0694(67)	0.1638(202)	0.0347(33)	0	0
O(4)	0.0186(18)	0.0186(18)	0.0492(47)	0.0093(9)	0	0
O(5)	0.3552(399)	0.0637(150)	0.2453(246)	0.1348(228)	− 0.2712(289)	− 0.0949(181)
O(6)	0.2137(1221)	0.1077(257)	0.3833(1336)	0.0766(554)	0.2621(1194)	0.1355(588)

probabilistic content of the state in Fig. 5d per unit cell is roughly $\frac{1}{4}$, the content $x/2$ of the Ca deficiency produced is equal to $\frac{1}{4}$; i.e., $x = \frac{1}{2}$. This relation means that the substitution of two CO_3 ions for the A sites introduces the substitution of one CO_3 ion for the B site when CAp crystals were grown by a $CaCO_3$ flux method.

4. SUMMARY

Carbonate apatite single crystals were grown by a $CaCO_3$ flux method. X-ray structure analyses indicated that the CO_3 ion randomly occupied six equivalent positions at the A site around the $\bar{6}$ axis; its triangular plane was parallel to the *c*-axis and one of C–O bonds lay on the $\bar{6}$ axis. The substitution of CO_3 ion in the A site is accompanied by compression of PO_4 tetrahedron along the *c*-axis and by extension of Ca(2) triangle located along the base of the CO_3 triangle. There exists a complex substitution mechanism between the A- and B-site CO_3 ions. One B-site substitution of CO_3 ion accompanies every two introductions of CO_3 ions in the A-site via the formation of $\frac{1}{2}$ Ca deficiency.

REFERENCES

1. R. A. Young, *J. Dent. Res.* [Suppl.] **53,** 193 (1974).
2. D. R. Simpson, *Clin. Orthop. Rel. Res.* **86,** 260 (1972).
3. G. Bonel and G. Montel, *C. R. Acad. Sci.* (*Paris*) **258,** 923 (1964).
4. Y. Suetsugu, I. Shimoya, and J. Tanaka, *J. Am. Ceram. Soc.* **81**(3), 746 (1998).
5. S. R. Hall, G. S. D. King, and J. M. Stewart, “Xtal 3.4 User’s Manual.” University of Western Australia, 1995.
6. J. A. Ibers and W. C. Hamilton, “International Tables for X-ray Crystallography,” Vol. IV. Kynoch Press, Birmingham, UK, 1974.
7. J. M. Hughes, M. Cameron, and K. D. Crowley, *Am. Mineral.* **74,** 870 (1989).
8. J. C. Elliott, “Structure and Chemistry of the Apatites and Other Calcium Orthophosphates.” Elsevier Science, Amsterdam, 1994.
9. J. C. Elliott, G. Bonel, and J. C. Trombe, *J. Appl. Crystallogr.* **13,** 618 (1980).
10. R. Z. LeGeros, *Nature* **206,** 403 (1965).
11. Y. Suetsugu and J. Tanaka, *J. Mater. Sci.* **10,** 561 (1999).